Margin Calibration for Long-Tailed Visual Recognition

Yidong Wang[1*], **Bowen Zhang**[1*], **Wenxin Hou**[2], **Zhen Wu**[3†], **Jindong Wang**[4†], **Takahiro Shinozaki**[1]

[1] *Tokyo Institute of Technology,* [2] *Microsoft STCA,* [3] *Nanjing University,* [4] *Microsoft Research Asia*

Editors: Emtiyaz Khan and Mehmet Gönen

Abstract

Long-tailed visual recognition tasks pose great challenges for neural networks on how to handle the imbalanced predictions between head (common) and tail (rare) classes, i.e., models tend to classify tail classes as head classes. While existing research focused on data resampling and loss function engineering, in this paper, we take a different perspective: the *classification margins*. We study the relationship between the margins and logits and empirically observe that the uncalibrated margins and logits are *positively correlated*. We propose a simple yet effective *MARgin Calibration* approach (**MARC**) to calibrate the margins to obtain better logits. We validate MARC through extensive experiments on common long-tailed benchmarks including CIFAR-LT, ImageNet-LT, Places-LT, and iNaturalist-LT. Experimental results demonstrate that our MARC achieves favorable results on these benchmarks. In addition, MARC is extremely easy to implement with just three lines of code. We hope this simple approach will motivate people to rethink the uncalibrated margins and logits in long-tailed visual recognition.

Keywords: Long-tailed learning; imbalanced classification

1. Introduction

Despite the great success of neural networks in the visual recognition field (Simonyan and Zisserman, 2014; He et al., 2016), it is still challenging for neural networks to deal with the ubiquitous long-tailed datasets in the real world (Yang et al., 2022; Buda et al., 2018; Kang et al., 2019; Zhou et al., 2020). To be clear, in the long-tailed datasets, the high-frequency classes (head/common classes) occupy most of the instances, whereas the low-frequency classes (tail/rare classes) involve a small amount of instances (Liu et al., 2019; Van Horn and Perona, 2017). Due to the imbalance of training data, the model performs well in head classes with much worse performance in tail classes (Buda et al., 2018; Zhang et al., 2021).

Towards addressing the long-tailed recognition problem, there are several strategies such as data re-sampling and loss function engineering. Data re-sampling aims to 'simulate' a balanced training dataset by over-sampling the tail class or under-sampling the head classes (Ando and Huang, 2017; Buda et al., 2018; Pouyanfar et al., 2018; Shen et al., 2016), while loss re-weighting is introduced to adjust the weights of losses for different classes or different instances (Byrd and Lipton, 2019; Khan et al., 2017; Wang et al., 2017). For more balanced gradients between classes, some class-balanced loss functions adjust the logits instead of weighting the losses (Menon et al., 2020; Cao et al., 2019b; Ren et al., 2020).

[†] Equal contribution.

[†] Corresponding to wuz@nju.edu.cn, jindong.wang@microsoft.com.

© 2022 Y. Wang, B. Zhang, W. Hou, Z. Wu, J. Wang & T. Shinozaki.

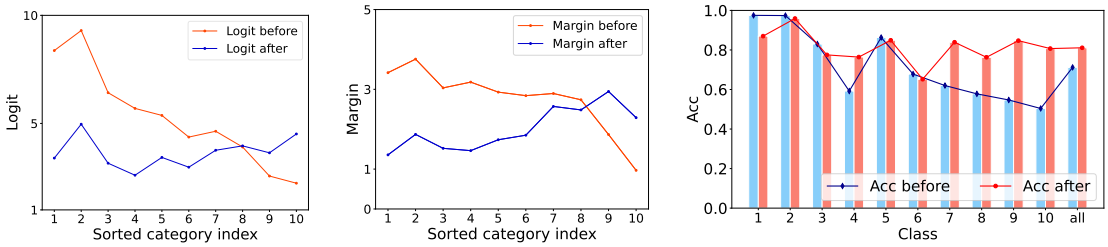

(a) Logits (b) Margins (c) Class-wise accuracy

Figure 1: **Logits, margins, and class-wise accuracy of CIFAR-10-LT with imbalance factor 200**. Here, the logit and margin represent the average logit and margin of each class, *before* and *after* refers to standard training and our method, respectively. The class indices are sorted by the number of samples (Head to tail).

However, as pointed out by existing research (Ganganwar, 2012; Zhou and Liu, 2005; Cao et al., 2019b), data re-sampling strategies and loss re-weighting schemes will possibly cause underfitting on the head class and overfitting on the tail class. On the other hand, class-balanced loss functions or data re-sampling will lead to worse data representations compared with the standard training using the cross-entropy loss and the instance-balanced sampling (i.e., each instance has the same probability of being sampled) (Kang et al., 2019; Ren et al., 2020). In addition, recent research reveals that the uncalibrated decision boundary given by the classifier head seems to be the performance bottleneck of the long-tailed visual recognition (Kang et al., 2019; Zhang et al., 2021). To benefit from both good data representations and the unbiased decision boundary, Decoupling, a heuristic two-stage strategy is proposed to adjust the initially-learned classifier head (Kang et al., 2019) after the standard training. Furthermore, distribution alignment (Zhang et al., 2021) is developed as an adaptive calibration function to adjust the initially trained logits for each data point. However, as pointed out by existing research (Platt et al., 1999; Elsayed et al., 2018), the margins and logits have a critical effect to the classification performance. *The relation between the uncalibrated margin and the logits is neglected in existing research*, where the margin is the distance from the data point to the decision boundary.

In this paper, we study the relationship between margins and logits, which are critical factors that dominate the long-tailed performance. As shown in Figure 1, we empirically find that the margin and the logit are correlated with the cardinality of each class. To be concrete, before any calibration, *head classes tend to have much larger margins and logits than tail classes*. Therefore, it is necessary to calibrate the margin to obtain the balanced logits. More importantly, as shown in Figure 1(c)subfigure, the uncalibrated margins and logits will have a negative impact on the classification performance. Therefore, it remains challenging to design an efficient method for such calibration that can achieve satisfying performance without introducing much computational burden.

The model can perform better with the confidence calibration (Platt et al., 1999; Guo et al., 2017; Zhang et al., 2021). however, in this work, we focus on calibrating the biased margins and propose a simple yet effective **MAR**gin **C**alibration (**MARC**) approach for long-tailed recognition. In detail, after getting the representations and the classifier head

from the standard training, we propose a simple class-specific margin calibration function with only $2K$ learnable parameters to adjust the initially learned margins, where K is the number of classes. As demonstrated in Figure 1, the logits are more balanced when using MARC. We conduct experiments on several popular long-tail benchmark datasets: CIFAR-10-LT (Krizhevsky et al., 2009), CIFAR-100-LT (Krizhevsky et al., 2009), Places-LT (Zhou et al., 2017), iNaturalist 2018 (Van Horn et al., 2018), and ImageNet-LT (Liu et al., 2019). The results demonstrate that our proposed MARC approach performs remarkably well while remaining very simple to implement. We hope that our exploration will attract attention to the imbalanced margins in long-tailed recognition.

To sum up, our contributions are as follows:

- For the first time in long-tailed recognition, we study the uncalibrated predictions from a margin-based perspective. We empirically find that uncalibrated margins will cause imperfect predictions, which could lead to future algorithm designs.
- Based on our observations, we propose a simple yet effective margin calibration (MARC) approach with only $2K$ trainable parameters to adjust the margins to get the unbiased prediction for long-tailed visual recognition problem.
- Compared with SOTA methods (Zhang et al., 2021; Hong et al., 2021), MARC is competitive on various long-tailed visual benchmarks like CIFAR-10-LT (Krizhevsky et al., 2009), CIFAR-100-LT (Krizhevsky et al., 2009), ImageNet-LT (Liu et al., 2019), Places-LT (Zhou et al., 2017) and iNaturalist2018 (Van Horn et al., 2018). In addition, it is extremely easy to implement with just three lines of code.

2. Related Work

Long-tailed visual recognition has attracted much attention for its commonness in the real world (Yang et al., 2022; He and Garcia, 2009; Buda et al., 2018; Kang et al., 2019; Ren et al., 2020; Yang and Xu, 2020; Hong et al., 2021). Existing methods can be divided into four categories.

Data re-sampling. Data re-sampling techniques re-sample the imbalanced training dataset to 'simulate' a balanced training dataset. These methods include under-sampling, over-sampling, and classed-balanced sampling. Under-sampling decreases the probability of the instance of head classes being sampled (Drummond et al., 2003), whereas over-sampling makes instances of tail classes more likely to be sampled (Chawla et al., 2002; Han et al., 2005; Wang et al., 2021a). Class-aware sampling chooses instances of each class with the same probabilities (Shen et al., 2016).

Loss function engineering. Loss function engineering is another direction to obtain balanced gradients during the training. The typical methods can be categorized as loss-reweighting and logits adjustment. Loss re-weighting adjusts the weights of losses for different classes or different instances in a more balanced manner, i.e. the instances in tail classes have larger weights than those in head classes (Byrd and Lipton, 2019; Khan et al., 2017; Wang et al., 2017). On the other hand, instead of re-weight losses, some class-balanced loss functions adjust the logits to get balanced gradients during training (Menon et al., 2020; Cao et al., 2019b; Ren et al., 2020; Yang et al., 2009).

Decision boundary adjustment. Nevertheless, data re-sampling or loss function engineering will influence the representations of data (Ren et al., 2020). Lots of empirical observations show that we can acquire good representation when using the standard training and the classifier head is the performance bottleneck (Kang et al., 2019; Zhang et al., 2021; Yu et al., 2020; Kim and Kim, 2020). To solve the above problem, decision boundary adjustment methods re-adjust the classifier head after the standard training in a learnable way (Kang et al., 2019; Zhang et al., 2021) or using maximum likelihood estimation such as the Platt scaling (Platt et al., 1999). However, they ignore the relationship between the uncalibrated margins and logits. Moreover, MARC targets a multi-class classification problem and Platting scaling targets binary classification (based on sigmoid), and their updating manners are also different since MARC adopts an end-to-end manner that updates $2K$ learnable parameters.

Other methods. There also exist other paradigms to deal with the long-tailed recognition task, including task-specific architecture design (Wang et al., 2021c; Zhou et al., 2020; Wang et al., 2021a), transfer learning (Liu et al., 2019; Yin et al., 2019), domain adaptation (Jamal et al., 2020), semi supervised learning and self supervised learning (Yang and Xu, 2020). But these methods either rely on the non-trivial architecture design or external data. In contrast, our proposed MARC is very simple to implement and does not require external data. Detailed comparison is shown in Table 1.

3. Method

3.1. Preliminaries

In the popular setting of long-tailed recognition (Kang et al., 2019; Cui et al., 2019; Ren et al., 2020), the training data distribution is imbalanced while the test data distribution is balanced. More formally, let $\mathcal{D} = \{(\mathbf{x}_i, y_i)\}_{i=1}^n$ be a training set, where y_i denotes the label of data point $\mathbf{x}_i$. Specifically, $n = \sum_{j=1}^K n_j$ is the total number of training samples, where n_j is the number of training samples in class j and K is the number of classes. We assume $n_1 > n_2 > \cdots > n_K$ without loss of generality. Normally, the prediction function is composed of two modules: the feature representation learning function $f : \mathbf{x} \mapsto \mathbf{z}$ parameterized by θ_r and the classifier $g : \mathbf{z} \mapsto y$ parameterized by θ_c, where $\mathbf{z} \in \mathbb{R}^p$ denotes the feature representation and p is the feature dimension. Typically, g is a linear classifier that gives the classification score of class j as:

$$\eta_j = g(\mathbf{z}) := \mathbf{W}_j \mathbf{z} + \mathbf{b}_j, \tag{1}$$

where $\mathbf{W}_j$ and $\mathbf{b}_j$ are the weight vector and bias for class j, respectively. Finally, using the softmax function, the probability of $\mathbf{x}_i$ being classified as label y_i is expressed as:

$$p(y = y_i | \mathbf{x}_i; \theta_r, \theta_c) = \frac{\exp(\eta_{y_i})}{\sum_{j=1}^K \exp(\eta_j)}, \tag{2}$$

and its loss is computed as the cross-entropy loss:

$$\ell(\mathbf{x}_i, y_i; \theta_r, \theta_c) = -\log\left(\frac{\exp(\eta_{y_i})}{\sum_{j=1}^K \exp(\eta_j)}\right). \tag{3}$$

3.2. Uncalibrated Margins and Logits

The decision boundary is often uncalibrated in long-tailed recognition, which will lead to imperfect predictions, i.e., the model tends to classify tail classes as head classes. To alleviate this issue, data re-sampling and loss function engineering are two directions to simulate a 'balanced' training dataset. However, such techniques will do harm to the representation learning of the model and lead to low overall accuracy (Kang et al., 2019; Ren et al., 2020). These methods including ours will sometimes do harm to the performance of head classes. However, the "good" performance of head classes is sometimes not always ensuring positive overall results. To benefit from both the good representation that will improve the overall accuracy and the calibrated decision boundary, decision boundary adjustment methods are developed (Kang et al., 2019; Zhang et al., 2021). However, existing decision boundary adjustment methods ignore such calibration in the margins, which is essential to avoid uncalibrated predictions. Thus, we aim to calibrate the margins to obtain balanced predictions.

In this paper, we find that the margins (Hastie et al., 2009) and logits are biased in long-tailed recognition. The margins are illustrated in Figure 2. We define an affine hyperplane $H_j \in \mathbb{R}^{p-1}$ of class j as $\mathbf{W}_j\mathbf{z} + \mathbf{b}_j = 0$, i.e. any representation point falling on the positive side of H_j can be attributed to class j. Assume that $\mathbf{z}_0$ is a point satisfying $\mathbf{W}_j\mathbf{z}_0 + \mathbf{b}_j = 0$, i.e., $\mathbf{z}_0$ is on the hyperplane H_j. Suppose $\mathbf{z}_1$ is an arbitrary point in the feature space. We construct the vector $\mathbf{z}_1 - \mathbf{z}_0$ pointing from $\mathbf{z}_0$ to $\mathbf{z}_1$ and project it onto the normal vector $\mathbf{W}_j$. The length of the projection vector $proj_{\mathbf{W}_j}(\mathbf{z}_1 - \mathbf{z}_0)$ is the margin from $\mathbf{z}_1$ to H_j. More formally, such margin is calculated as:

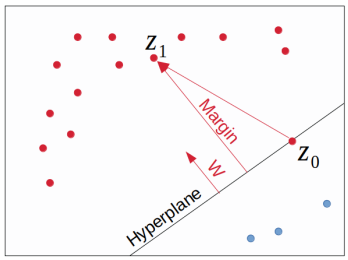

Figure 2: **Illustration of margins.** The red and blue dots denote majority and minority classes, respectively.

$$
\begin{aligned}
d_j &= \left\| proj_{\mathbf{W}_j}(\mathbf{z}_1 - \mathbf{z}_0) \right\| \\
&= \left\| \frac{\mathbf{W}_j \cdot (\mathbf{z}_1 - \mathbf{z}_0)}{\mathbf{W}_j \cdot \mathbf{W}_j} \mathbf{W}_j \right\| \\
&= \frac{\mathbf{W}_j \cdot \mathbf{z}_1 - \mathbf{W}_j \cdot \mathbf{z}_0}{\|\mathbf{W}_j\|} \\
&= \frac{\mathbf{W}_j \mathbf{z}_1 + \mathbf{b}_j}{\|\mathbf{W}_j\|} \quad (\text{since } \mathbf{W}_j\mathbf{z}_0 + \mathbf{b}_j = 0),
\end{aligned} \tag{4}
$$

where $\|\cdot\|$ denotes L2 norm. Thus, the logit $\mathbf{W}_j \cdot \mathbf{z}_1 + \mathbf{b}_j$ can also be expressed as $\|\mathbf{W}_j\| d_j$. Based on this conclusion, we can rewrite (2) as:

$$
p(y = y_i | \mathbf{x}_i; \theta_r, \theta_c) = \frac{\exp(\eta_{y_i})}{\sum_{j=1}^{K} \exp(\eta_j)} = \frac{\exp(\|\mathbf{W}_{y_i}\| d_{y_i})}{\sum_{j=1}^{K} \exp(\|\mathbf{W}_j\| d_j)}. \tag{5}
$$

Consider a data point is on the decision boundary of class j and class t (on the hyperplane in Figure 2), i.e., such data point has the same probability of being classified as class j or class t. Clearly, the assumed data point on the decision boundary satisfies:

$$
\eta_j = \eta_t = \|\mathbf{W}_j\| d_j = \|\mathbf{W}_t\| d_t. \tag{6}
$$

According to (6), data will be classified as class t because $d_j < d_t$ when $\|\mathbf{W}_j\| = \|\mathbf{W}_t\|$. And our empirical observations show that head classes tend to have much larger margins and logits than tail classes:

$$\begin{aligned} &\bar{d}_1 > \bar{d}_2 > \cdots > \bar{d}_K, \\ &\bar{\eta}_1 > \bar{\eta}_2 > \cdots > \bar{\eta}_K, \\ &\text{if} \quad n_1 > n_2 > \cdots > n_K, \end{aligned} \tag{7}$$

where $\bar{d}_j$ and $\bar{\eta}_j$ are the average margin and logit of class j after the standard training, respectively. In detail, on sub-dataset $\mathcal{D}_j = \{(\mathbf{x}_i, y_i = j)\}_{i=1}^{n_j}$, $\bar{\eta}_j = \frac{1}{n_j}\eta_j$, $\bar{d}_j = \frac{\bar{\eta}_j}{\|\mathbf{W}_j\|}$.

3.3. Margin Calibration (MARC)

To get the calibrated logits, we propose MARC to calibrate the margins after the standard training. Concretely speaking, we train a simple class-specific margin calibration model with the original margin fixed:

$$\hat{d}_j = \omega_j \cdot d_j + \beta_j, \tag{8}$$

where ω_j and β_j are learnable parameters for class j and $j \in [1, K]$. It is worth noting that MARC is extended from class j to the whole dataset in practise. In other words, MARC only has $2K$ trainable parameters. Thus, the calibrated logit is computed as:

$$\begin{aligned} \|\mathbf{W}_j\|\hat{d}_j &= \|\mathbf{W}_j\|(\omega_j \cdot d_j + \beta_j) \\ &= \omega_j \cdot \|\mathbf{W}_j\| d_j + \beta_j \cdot \|\mathbf{W}_j\| \\ &= \omega_j \cdot \eta_j + \beta_j \cdot \|\mathbf{W}_j\|, \end{aligned} \tag{9}$$

where η_j is the initial fixed logit. Then, we can get the calibrated prediction distribution:

$$p(y = y_i|\mathbf{x}_i; \theta_r, \theta_c) = \frac{\exp(\omega_{y_i} \cdot \eta_{y_i} + \beta_{y_i} \cdot \|\mathbf{W}_{y_i}\|)}{\sum_{j=1}^{K} \exp(\omega_j \cdot \eta_j + \beta_j \cdot \|\mathbf{W}_j\|)}. \tag{10}$$

The training process of the margin calibration approach can be written with *just three* lines of Pytorch codes as shown in Line 4-6 of Algorithm 1.

Algorithm 1 The torch-like code for MARC.

1: Initialization of the margin calibration approach:
```
omega=torch.nn.Parameter(torch.ones(1,K))
beta=torch.nn.Parameter(torch.zeros(1,K))
```
2: **Input:** training data x, standard pre-trained neural network model.
```
3: with torch.no_grad():
4:     w_norm = torch.norm(model.fc.weight, dim=1)
5:     logit_before = model(x)
6: logit_after = omega * logit_before + beta * w_norm
```
7: Compute loss and update parameters of omega and beta.

Furthermore, for more balanced gradients during training, we re-weight the loss as the previous work does (Zhang et al., 2021). Finally, the loss for training the margin calibration approach is:

$$\ell(\mathbf{x}_i, y_i; \tilde{\theta}_r, \tilde{\theta}_c, \omega, \beta) = -U_{y_i} \cdot \log \left(\frac{\exp\left(\omega_{y_i} \cdot \eta_{y_i} + \beta_{y_i} \cdot \|\mathbf{W}_{y_i}\|\right)}{\sum_{j=1}^{K} \exp(\omega_j \cdot \eta_j + \beta_j \cdot \|\mathbf{W}_j\|)} \right), \tag{11}$$

where $\tilde{\theta}_r$ and $\tilde{\theta}_c$ denote that these parameters are frozen during training. The weight for class y_i is calculated as:

$$U_{y_i} = K \cdot \frac{(1/n_{y_i})^{\gamma}}{\sum_{j=1}^{K} (1/n_j)^{\gamma}}, \tag{12}$$

where γ is a scale hyper-parameter. When $\gamma = 0$, the weight for all classes is 1, which means no re-weighting at all.

To be more clear, the whole detailed training procedure including both standard training and margin calibration function training is demonstrated in Algorithm 2. Lines 2-6 include the training procedure of the standard training using the instance-balanced sampling and the cross-entropy loss. Lines 7-11 contain the training process of our margin calibration function. It is worth noting that in the second stage, parameters θ_r and θ_c are all fixed.

3.4. Discussion

We clarify the differences between MARC and other learnable decision boundary adjustment methods in detail. As shown in Table 1, Decouple-cRT (Kang et al., 2019) retrains the whole parameters of the classifier, while Decouple-LWS (Kang et al., 2019) only adjusts the norm of weight vectors $\|\mathbf{W}_j\|$. Instead of adjusting the classifier head, DisAlign (Zhang et al., 2021) chooses to calibrate the logit for each data point. But their calibration method is heuristic that simply adds the calibrated logit and the original logit with a re-weighting scheme. To be more clear, the weighted sum of logits for DisAlign is $\sigma(\mathbf{z}_j)(\omega_j \eta_j + \beta) + (1 - \sigma(\mathbf{z}_j))\eta_j$, where $\sigma(\cdot)$ is an instance-specific confidence function. However, different from previous methods, our MARC focuses on calibrating the margin which we believe is the performance bottleneck of the long-tailed classifier.

Table 1: The difference between MARC and other decision boundary adjustment methods. $j \in [1, K]$ is class index.

Method	calibration method
Decouple-cRT (Kang et al., 2019)	retrain $\mathbf{W}_j, \mathbf{b}_j$
Decouple-LWS (Kang et al., 2019)	$\|\mathbf{W}_j\|^{1-\omega_j}$
DisAlign (Zhang et al., 2021)	$\sigma(\mathbf{z}_j)(\omega_j \eta_j + \beta) + (1 - \sigma(\mathbf{z}_j))\eta_j$
MARC	$\omega_j \cdot d_j + \beta_j$

4. Experiments

In this section, we conduct extensive experiments compared with the state-of-the-art methods to validate the effectiveness of MARC. First, we report performance on common bench-

Algorithm 2 The detailed training procedure including both standard training and margin calibration function training.

1: **Input:** The training dataset $\mathcal{D} = \{(\mathbf{x}_i, y_i)\}_{i=1}^{n}$, the parameters of the representation function θ_r, the parameters of the classifier θ_c, parameters of the margin calibration function ω and β, number of classes K and the pre-defined scale hyper-parameter γ.
2: First stage: the standard training use the instance-balanced sampling and the cross entropy loss.
3: **while** not reach the maximum iteration **do**
4: Use instance-balanced sampling to sample a batch of data $\mathcal{D}_s = \{(\mathbf{x}_i, y_i)\}_{i=1}^{s}$ from the training dataset $\mathcal{D}$, where s is the batch size.
5: Compute the loss and update the model parameters.
$\ell(\mathcal{D}_s; \theta_r, \theta_c) = \frac{-1}{s} \sum_{i=1}^{s} \log \left(\frac{\exp(\eta_{y_i})}{\sum_{j=1}^{K} \exp(\eta_j)} \right)$, where η_j is classification score of class j.
6: **end while**
7: Second stage: Calibrate the margins trained in the first stage.
8: **while** not reach the maximum iteration **do**
9: Use instance-balanced sampling to sample a batch of data $\mathcal{D}_s = \{(\mathbf{x}_i, y_i)\}_{i=1}^{s}$ from the training dataset $\mathcal{D}$, where s is the batch size.
10: Compute the loss and update the model parameters.
$\ell(\mathcal{D}_s; \tilde{\theta}_r, \tilde{\theta}_c, \omega, \beta) = \frac{1}{s} \sum_{i=1}^{s} (-U_{y_i} \cdot \log \left(\frac{\exp(\omega_{y_i} \cdot \eta_{y_i} + \beta_{y_i} \cdot \|\mathbf{W}_{y_i}\|)}{\sum_{j=1}^{K} \exp(\omega_j \cdot \eta_j + \beta_j \cdot \|\mathbf{W}_j\|)} \right)$, where parameters with $\tilde{\cdot}$ are fixed during training and U_j is calculated as shown in Eq. 12.
11: **end while**
12: **Return:** Model parameters $\theta_r, \theta_c, \omega, \beta$.

marks like CIFAR-LT (Krizhevsky et al., 2009), ImageNet-LT (Liu et al., 2019), Places-LT (Zhou et al., 2017) and iNaturalist2018 (Van Horn et al., 2018). The results of MARC are competitive even though MARC is simple. Then we conduct further analysis to explain the reason for the success of MARC.

4.1. Setup

Datasets We follow the common evaluation protocol (Liu et al., 2019) and conduct experiments on CIFAR-10-LT (Krizhevsky et al., 2009), CIFAR-100-LT (Krizhevsky et al., 2009), ImageNet-LT (Liu et al., 2019), Places-LT (Zhou et al., 2017) and iNaturalist2018 (Van Horn et al., 2018). The imbalance factor used in CIFAR datasets is defined as N_{max}/N_{min} where N_{max} is the number of samples on the largest class and N_{min} the smallest. We report CIFAR results with two different imbalance ratios: 100 and 200. For ImageNet-LT and Places-LT experiments, we further split classes into three sets: Many-shot (with more than 100 images), Medium-shot (with 20 to 100 images), and Few-shot (with less than 20 images).

Training Configuration For a fair comparison, our experiments are conducted under the most commonly used codebase of long-tailed studies: Open Long-Tailed Recognition (OLTR) (Liu et al., 2019), using PyTorch (Paszke et al., 2019) framework. The model structures used for CIFAR, ImageNet-LT, Places-LT and iNaturalist18 datasets are ResNet32, ResNeXt50, ResNet152 and ResNet50, respectively. The model for Places-LT is pre-trained

on the full ImageNet-2012 dataset while models for other datasets are trained from scratch. For ImageNet-LT, Places-LT, and iNaturalist18, we train 90, 30, and 200 epochs in the first standard training stage; and 10, 10, and 30 epochs in the second margin calibration stage, with the batch size of 256, 128, and 256, respectively. For CIFAR-10-LT and CIFAR-100-LT, the models are trained for 13,000 iterations with a batch size of 512. We use the SGD optimizer with momentum 0.9 and weight decay $5e-4$ for all datasets except for iNaturalist18 where the weight decay is $1e-4$. In the standard training stage, we use a cosine learning rate schedule with an initial value of 0.05 for CIFAR and 0.1 for other datasets, which gradually decays to 0. In the margin calibration stage, we use a cosine learning rate schedule with an initial learning rate starting from 0.05 to 0 for all datasets. γ is set to 1.2 for all datasets. The hyper-parameters of compared methods follow their paper. *For fairness, we use the same pre-trained model for decision boundary adjustment methods.*

Table 2: Accuracy on CIFAR-LT.

Dataset	CIFAR-10-LT		CIFAR-100-LT	
Imbalance Factor	100	200	100	200
Softmax	78.7	74.4	45.3	41.0
Data Re-sampling				
Class Balanced Sampling (CBS)	77.8	68.3	42.6	37.8
Loss Function Engineering				
Class Balanced Weighting (CBW)	78.6	72.5	42.3	36.7
Class Balanced Loss (Cui et al., 2019)	78.2	72.6	44.6	39.9
Focal Loss (Lin et al., 2017)	77.1	71.8	43.8	40.2
LADE (Hong et al., 2021)	81.8	76.9	45.4	43.6
LDAM (Cao et al., 2019a)	78.9	73.6	46.1	41.3
Equalization Loss (Tan et al., 2020)	78.5	74.6	47.4	43.3
Balanced Softmax (Ren et al., 2020)	83.1	79.0	50.3	45.9
Decision Boundary Adjustment				
DisAlign (Zhang et al., 2021)	78.0	71.2	49.1	43.6
Decouple-cRT (Kang et al., 2019)	82.0	76.6	50.0	44.5
Decouple-LWS (Kang et al., 2019)	83.7	78.1	50.5	45.3
Others				
BBN (Zhou et al., 2020)	79.8	-	42.6	-
Hybrid-SC (Wang et al., 2021c)	81.4	-	46.7	-
MARC	**85.3**	**81.1**	**50.8**	**47.4**

Table 3: Accuracy on iNaturalist-LT.

Method	Top-1 Accuracy
Softmax	65.0
Loss Function Engineering	
Class Balanced Loss (Cui et al., 2019)	61.1
LDAM (Cao et al., 2019b)	64.6
Balanced Softmax (Ren et al., 2020)	69.8
LADE (Hong et al., 2021)	70.0
Decision Boundary Adjustment	
Decouple-π-norm (Kang et al., 2019)	69.3
Decouple-LWS (Kang et al., 2019)	69.5
DisAlign (Zhang et al., 2021)	70.3
Others	
Casual Norm (Tang et al., 2020)	63.9
Hybrid-SC (Wang et al., 2021c)	68.1
MARC	**70.4**

4.2. Comparison with previous methods

In this section, we compare the performance of MARC to other recent works. We select some recent methods from each of the following four categories for comparison: data re-sampling, loss function engineering, decision boundary adjustment, and others. The standard training with the cross-entropy loss and instance balance sampling is called Softmax in our results.

CIFAR Table 2 presents results for CIFAR-10-LT and CIFAR-100-LT. MARC outperforms all other methods in CIFAR-LT. Compared with other decision boundary adjustment methods, MARC shows favorable results. The accuracy of MARC outruns Decouple-LWS 1.6%, 3%, 0.3% and 1.9% on CIFAR-10-LT(100), CIFAR-10-LT(200), CIFAR-100-LT(100) and CIFAR-100-LT(200) respectively, where $(\cdot)$ denotes the imbalance factor. In addition, MARC outperforms all data re-sampling and loss function engineering methods that my need laborious hyper-parameter. The performance of well-designed networks such as BBN and Hybrid-SC are also not as good as that of MARC.

ImageNet-LT We further evaluate MARC on the ImageNet-LT dataset. As Table 4 shows, MARC is better than all loss function engineering methods. Compared with LADE, although our overall accuracy is 0.4% higher, the accuracy on the few-shot classes is 5.4% higher. The few-shot accuracy and overall accuracy of MARC are 1.9% and 0.1% higher than DisAlign respectively. Our results are quite surprising considering the simplicity of MARC (See next section for time comparison).

Table 4: Accuracy on ImageNet-LT.

Method	Many	Medium	Few	Overall
Softmax	65.1	35.7	6.6	43.1
Loss Function Engineering				
Focal Loss (Lin et al., 2017)	64.3	37.1	8.2	43.7
Seesaw (Wang et al., 2021b)	**67.1**	45.2	21.4	50.4
Balanced Softmax (Ren et al., 2020)	62.2	48.8	29.8	51.4
LADE (Hong et al., 2021)	62.3	49.3	31.2	51.9
Decision Boundary Adjustment				
Decouple-π-norm (Kang et al., 2019)	59.1	46.9	30.7	49.4
Decouple-cRT (Kang et al., 2019)	61.8	46.2	27.4	49.6
Decouple-LWS (Kang et al., 2019)	60.2	47.2	30.3	49.9
DisAlign (Zhang et al., 2021)	60.8	**50.4**	34.7	52.2
Others				
OLTR (Liu et al., 2019)	51.0	40.8	20.8	41.9
Causal Norm (Tang et al., 2020)	62.7	48.8	31.6	51.8
MARC	60.4	50.3	**36.6**	**52.3**

Table 5: Accuracy on Places-LT

Method	Many	Medium	Few	Overall
Softmax	46.4	27.9	12.5	31.5
Loss Function Engineering				
Focal Loss (Lin et al., 2017)	41.1	34.8	22.4	34.6
Balanced Softmax (Ren et al., 2020)	42.0	38.0	17.2	35.4
LADE (Hong et al., 2021)	42.8	39.0	31.2	**38.8**
Decision Boundary Adjustment				
Decouple-LWS (Kang et al., 2019)	40.6	39.1	28.6	37.6
Decouple-π-norm (Kang et al., 2019)	37.8	**40.7**	31.8	37.9
DisAlign (Zhang et al., 2021)	40.0	39.6	32.3	38.3
Others				
OLTR (Liu et al., 2019)	**44.7**	37.0	25.3	35.9
Causal Norm (Tang et al., 2020)	23.8	35.8	**40.4**	32.4
MARC	39.9	39.8	32.6	38.4

Places-LT For the Places-LT dataset, MARC achieves better performance than other decision boundary adjustment methods. Though our overall accuracy is lower than LADE, our few-shot accuracy is still 1.4% higher than LADE. Though MARC is not the best in Places-LT, the results of MARC are still competitive compared with other methods.

iNaturalist-LT Finally, we present the Top-1 accuracy results for iNaturalist-LT dataset in Table 3. We can observe a similar trend that our proposed method wins all the existing approaches and surpasses DisAlign by 0.1% absolute improvement.

4.3. Effectiveness validation

Comparison of the trainable parameters of decision boundary adjustment methods As shown in Table 6, MARC achieves the best performance among other compared methods on CIFAR-100-LT(200) and ImageNet-LT. Even though our trainable parameters are more than Decouple-LWS, our performance is better. Besides, it is surprising that MARC obtains such a favorable performance with only so few parameters.

Table 6: **Comparison of the trainable parameters (#Param.) of the learnable decision boundary adjustment methods.** p is the feature dimension and K is the number of classes (ResNeXt50 for ImageNet-LT: $p = 2048, K = 1000$).

Method	CIFAR-100-LT	ImageNet-LT	#Param.
Decouple-cRT	44.5	49.6	$pK + K$
Decouple-LWS	45.3	49.9	K
DisAlign	43.6	52.2	$p + 2K$
MARC	**47.4**	**52.3**	$2K$

Effects of different standard pre-trained model We use different standard pre-trained models on CIFAR-100-LT(200) to explore their effects. As Table 7 illustrates, as the pre-trained dataset gets more balanced, the performance of our margin calibration method gets better. This shows that when comparing decision boundary methods, using the same standard training model is very important for fairness. And the codebase will also affect the standard training. *This is the reason why the result of DisAlign in our paper is inconsistent with the original paper since we cannot get the same standard pre-trained model they used.* So instead, we use our own standard pre-trained model for MARC and DisAlign for fairness. Table 7 also demonstrates that the margin calibration method can achieve better performance when given better representations. So our future works include how to get better representations.

Table 7: Top-1 accuracy on CIFAR-100-LT(200) with different standard pre-trained models.

Standard pre-trained dataset	Top-1 Accuracy
CIFAR-100-LT(200)	47.1
CIFAR-100-LT(100)	50.7
CIFAR-100-LT(50)	54.5

4.4. Further analysis

In this section, we conduct different experiments for further analysis. To be concrete, we empirically show that MARC can achieve more balanced margins and logits compared with DisAlign. Moreover, the class-wise accuracy of MARC is much better than the standard training baseline model on CIFAR-LT, which indicates that we can alleviate the imbalanced prediction problem and reduce the performance gap between the head and the tail classes.

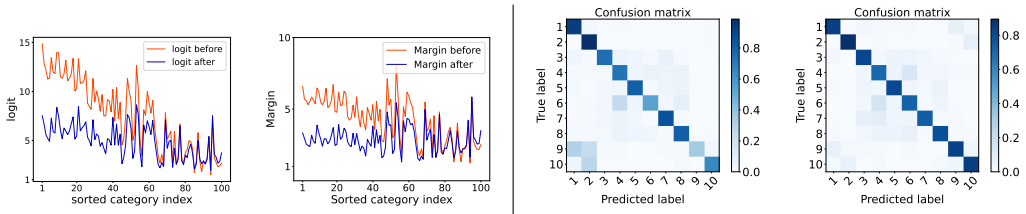

(*a*) Logits (*b*) Margins (*c*) Standard training. (*d*) MARC

Figure 3: (a) and (b): **Logits and margins of CIFAR-100-LT(200)**. Here, the logit and margin represent the average logit and margin of each class, *before* refers to the standard training results and *after* refers to the results after our calibration method. The class indices are sorted by the number of samples (Head to tail). (c) and (d): **Confusion matrix of the standard training and MARC on long-tailed CIFAR-10-LT(200).** The fading color of diagonal elements refers to the disparity of the accuracy.

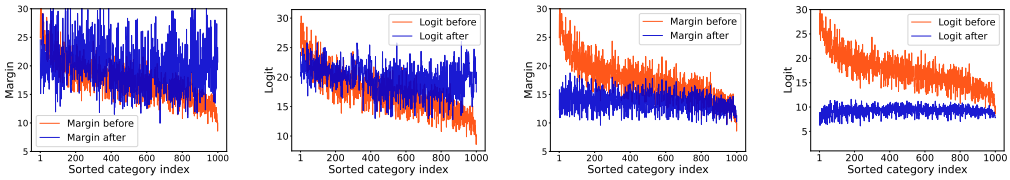

(a) Margins of DisAlign. (b) Logits of DisAlign. (c) Margins of MARC. (d) Logits of MARC.

Figure 4: **The values of margins and logits for each class on the ImageNet-LT dataset.** The logit and margin represent the average logit and margin of each class. The class indices are sorted by the number of samples (Head to tail). *Before* refers to the standard training results and *after* refers to the results after using the decision boundary adjustment method.

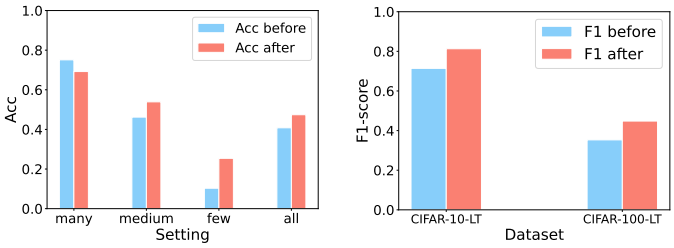

(a) CIFAR-100-LT(200). (b) F1 scores on CIFAR-LT.

Figure 5: The detailed performance of CIFAR-100-LT(200). *Before* refers to the standard training results and *after* refers to the results after MARC.

Visualization of the margin and logit In this subsection, we visualize the values of margins and logits for each class to show the effect of MARC. As illustrated both in Figure 3, Figure 4(c)subfigure and Figure 4(d)subfigure, before margin calibration, the margins and the logits are uncalibrated, i.e. the head classes tend to have much larger margins and logits than tail classes. We believe the bias in margins and logits will lead to imperfect predictions in long-tailed visual recognition. The margins and logits become more balanced after the margin calibration. This result proves that we can get better predictions by calibrating the margin. Moreover, as shown in Figure 4(a)subfigure and Figure 4(b)subfigure, MARC will obtain more balanced margins and gradients than DisAlign. The instability of DisAlign may be caused by their heuristic design of the combination of the calibrated logits and the origin logits.

Class-wise performance on CIFAR-LT As we can see in Figure 3(c)subfigure and 3(d)subfigure, after our margin calibration method, the performance on tail classes is improved while that on head classes is not severely affected. More intuitively, Figure 5 shows the class-wise performance. The accuracy of the tail class is much higher than that of the head class. The performance degradation on head classes may be caused by the false pos-

itive predictions on head classes, i.e., the standard training method tends to classify tail classes as head classes, resulting in high accuracy on the head classes. The bad performance on tail classes when using standard training also proves this. In addition, the overall accuracy and F1-score show that MARC alleviates the uncalibrated prediction problem.

Effects of different γ To explore the effect of different γ, we also conduct experiments and visualize the performances on all CIFAR-100-LT(200). The results are shown in Figure 6. We can observe that compared 1.2 is the best compared with other values. γ can not be too large since in this way the weight for head classes is too small. It is worth noting that MARC also achieves 45.2% accuracy when γ is 0. This means MARC still works even if we do not use any loss re-weighting techniques in the second stage. For other datasets, we directly use 1.2 for γ.

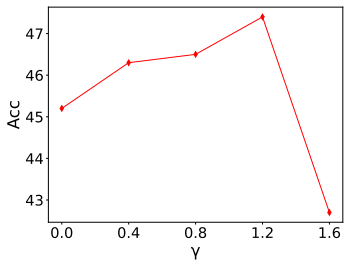

Figure 6: Accuracy on CIFAR-100-LT(200) with different γ.

5. Conclusions

This paper studied the long-tailed visual recognition problem. Specifically, we found that head classes tend to have much larger margins and logits than tail classes. Motivated by our findings, we proposed a margin calibration function with only $2K$ learnable parameters to obtain the balanced logits in long-tailed visual recognition. Even though our method is very simple to implement, extensive experiments show that MARC achieves favorable results compared with previous methods without altering the model representation. We hope that our study on logits and margins could provide experience for joint optimization of the model representation and margin calibration.In the future, we aim to develop a unified theory to better support our algorithm design and apply this algorithm to more long-tailed applications.

Acknowledgments

We would like to thank anonymous reviewers for their insightful suggestions to help improve the paper. This study was supported by JSPS KAKENHI Grand Number JP22K12069.

References

Shin Ando and Chun Yuan Huang. Deep over-sampling framework for classifying imbalanced data. In *ECML-PKDD*, pages 770–785. Springer, 2017.

Mateusz Buda, Atsuto Maki, and Maciej A Mazurowski. A systematic study of the class imbalance problem in convolutional neural networks. *Neural Networks*, 106:249–259, 2018.

Jonathon Byrd and Zachary Lipton. What is the effect of importance weighting in deep learning? In *ICML*, pages 872–881. PMLR, 2019.

Kaidi Cao, Colin Wei, Adrien Gaidon, Nikos Arechiga, and Tengyu Ma. Learning imbalanced datasets with label-distribution-aware margin loss. *arXiv preprint arXiv:1906.07413*, 2019a.

Kaidi Cao, Colin Wei, Adrien Gaidon, Nikos Arechiga, and Tengyu Ma. Learning imbalanced datasets with label-distribution-aware margin loss. In *NeurIPS*, 2019b.

Nitesh V Chawla, Kevin W Bowyer, Lawrence O Hall, and W Philip Kegelmeyer. Smote: synthetic minority over-sampling technique. *Journal of artificial intelligence research*, 16: 321–357, 2002.

Yin Cui, Menglin Jia, Tsung-Yi Lin, Yang Song, and Serge Belongie. Class-balanced loss based on effective number of samples. In *CVPR*, pages 9268–9277, 2019.

Chris Drummond, Robert C Holte, et al. C4. 5, class imbalance, and cost sensitivity: why under-sampling beats over-sampling. In *Workshop on learning from imbalanced datasets II*, volume 11, pages 1–8. Citeseer, 2003.

Gamaleldin Elsayed, Dilip Krishnan, Hossein Mobahi, Kevin Regan, and Samy Bengio. Large margin deep networks for classification. *NeurIPS*, 31, 2018.

Vaishali Ganganwar. An overview of classification algorithms for imbalanced datasets. *International Journal of Emerging Technology and Advanced Engineering*, 2(4):42–47, 2012.

Chuan Guo, Geoff Pleiss, Yu Sun, and Kilian Q Weinberger. On calibration of modern neural networks. In *ICML*, pages 1321–1330. PMLR, 2017.

Hui Han, Wen-Yuan Wang, and Bing-Huan Mao. Borderline-smote: a new over-sampling method in imbalanced data sets learning. In *International conference on intelligent computing*, pages 878–887. Springer, 2005.

Trevor Hastie, Robert Tibshirani, Jerome H Friedman, and Jerome H Friedman. *The elements of statistical learning: data mining, inference, and prediction*, volume 2. Springer, 2009.

Haibo He and Edwardo A Garcia. Learning from imbalanced data. *IEEE TKDE*, 21(9): 1263–1284, 2009.

Kaiming He, Xiangyu Zhang, Shaoqing Ren, and Jian Sun. Deep residual learning for image recognition. In *CVPR*, pages 770–778, 2016.

Youngkyu Hong, Seungju Han, Kwanghee Choi, Seokjun Seo, Beomsu Kim, and Buru Chang. Disentangling label distribution for long-tailed visual recognition. In *CVPR*, pages 6626–6636, 2021.

Muhammad Abdullah Jamal, Matthew Brown, Ming-Hsuan Yang, Liqiang Wang, and Boqing Gong. Rethinking class-balanced methods for long-tailed visual recognition from a domain adaptation perspective. In *CVPR*, pages 7610–7619, 2020.

Bingyi Kang, Saining Xie, Marcus Rohrbach, Zhicheng Yan, Albert Gordo, Jiashi Feng, and Yannis Kalantidis. Decoupling representation and classifier for long-tailed recognition. In *ICML*, 2019.

Salman H Khan, Munawar Hayat, Mohammed Bennamoun, Ferdous A Sohel, and Roberto Togneri. Cost-sensitive learning of deep feature representations from imbalanced data. *IEEE TNNLS*, 29(8):3573–3587, 2017.

Byungju Kim and Junmo Kim. Adjusting decision boundary for class imbalanced learning. *IEEE Access*, 8:81674–81685, 2020.

Alex Krizhevsky, Geoffrey Hinton, et al. Learning multiple layers of features from tiny images. 2009.

Tsung-Yi Lin, Priya Goyal, Ross Girshick, Kaiming He, and Piotr Dollár. Focal loss for dense object detection. In *ICCV*, pages 2980–2988, 2017.

Ziwei Liu, Zhongqi Miao, Xiaohang Zhan, Jiayun Wang, Boqing Gong, and Stella X Yu. Large-scale long-tailed recognition in an open world. In *CVPR*, pages 2537–2546, 2019.

Aditya Krishna Menon, Sadeep Jayasumana, Ankit Singh Rawat, Himanshu Jain, Andreas Veit, and Sanjiv Kumar. Long-tail learning via logit adjustment. In *ICLR*, 2020.

Adam Paszke, Sam Gross, Francisco Massa, Adam Lerer, James Bradbury, Gregory Chanan, Trevor Killeen, Zeming Lin, Natalia Gimelshein, Luca Antiga, et al. Pytorch: An imperative style, high-performance deep learning library. *NeurIPS*, 32:8026–8037, 2019.

John Platt, Nello Cristianini, and John Shawe-Taylor. Large margin dags for multiclass classification. *NIPS*, 12, 1999.

Samira Pouyanfar, Yudong Tao, Anup Mohan, Haiman Tian, Ahmed S Kaseb, Kent Gauen, Ryan Dailey, Sarah Aghajanzadeh, Yung-Hsiang Lu, Shu-Ching Chen, et al. Dynamic sampling in convolutional neural networks for imbalanced data classification. In *2018 IEEE conference on multimedia information processing and retrieval (MIPR)*, pages 112–117. IEEE, 2018.

Jiawei Ren, Cunjun Yu, Shunan Sheng, Xiao Ma, Haiyu Zhao, Shuai Yi, and Hongsheng Li. Balanced meta-softmax for long-tailed visual recognition. *arXiv preprint arXiv:2007.10740*, 2020.

Li Shen, Zhouchen Lin, and Qingming Huang. Relay backpropagation for effective learning of deep convolutional neural networks. In *ECCV*, pages 467–482. Springer, 2016.

Karen Simonyan and Andrew Zisserman. Very deep convolutional networks for large-scale image recognition. *arXiv preprint arXiv:1409.1556*, 2014.

Jingru Tan, Changbao Wang, Buyu Li, Quanquan Li, Wanli Ouyang, Changqing Yin, and Junjie Yan. Equalization loss for long-tailed object recognition. In *CVPR*, pages 11662–11671, 2020.

Kaihua Tang, Jianqiang Huang, and Hanwang Zhang. Long-tailed classification by keeping the good and removing the bad momentum causal effect. *NeurIPS*, 33, 2020.

Grant Van Horn and Pietro Perona. The devil is in the tails: Fine-grained classification in the wild. *arXiv preprint arXiv:1709.01450*, 2017.

Grant Van Horn, Oisin Mac Aodha, Yang Song, Yin Cui, Chen Sun, Alex Shepard, Hartwig Adam, Pietro Perona, and Serge Belongie. The inaturalist species classification and detection dataset. In *CVPR*, pages 8769–8778, 2018.

Jianfeng Wang, Thomas Lukasiewicz, Xiaolin Hu, Jianfei Cai, and Zhenghua Xu. Rsg: A simple but effective module for learning imbalanced datasets. In *CVPR*, pages 3784–3793, 2021a.

Jiaqi Wang, Wenwei Zhang, Yuhang Zang, Yuhang Cao, Jiangmiao Pang, Tao Gong, Kai Chen, Ziwei Liu, Chen Change Loy, and Dahua Lin. Seesaw loss for long-tailed instance segmentation. In *CVPR*, pages 9695–9704, 2021b.

Peng Wang, Kai Han, Xiu-Shen Wei, Lei Zhang, and Lei Wang. Contrastive learning based hybrid networks for long-tailed image classification. In *CVPR*, pages 943–952, 2021c.

Yu-Xiong Wang, Deva Ramanan, and Martial Hebert. Learning to model the tail. In *NeurIPS*, pages 7032–7042, 2017.

Chan-Yun Yang, Jr-Syu Yang, and Jian-Jun Wang. Margin calibration in svm class-imbalanced learning. *Neurocomputing*, 73(1-3):397–411, 2009.

Lu Yang, He Jiang, Qing Song, and Jun Guo. A survey on long-tailed visual recognition. *IJCV*, pages 1–36, 2022.

Yuzhe Yang and Zhi Xu. Rethinking the value of labels for improving class-imbalanced learning. In *NeurIPS*, 2020.

Xi Yin, Xiang Yu, Kihyuk Sohn, Xiaoming Liu, and Manmohan Chandraker. Feature transfer learning for face recognition with under-represented data. In *CVPR*, 2019.

Haiyang Yu, Ningyu Zhang, Shumin Deng, Zonggang Yuan, Yantao Jia, and Huajun Chen. The devil is the classifier: Investigating long tail relation classification with decoupling analysis. *arXiv preprint arXiv:2009.07022*, 2020.

Songyang Zhang, Zeming Li, Shipeng Yan, Xuming He, and Jian Sun. Distribution alignment: A unified framework for long-tail visual recognition. In *CVPR*, 2021.

Bolei Zhou, Agata Lapedriza, Aditya Khosla, Aude Oliva, and Antonio Torralba. Places: A 10 million image database for scene recognition. *IEEE TPAMI*, 40(6):1452–1464, 2017.

Boyan Zhou, Quan Cui, Xiu-Shen Wei, and Zhao-Min Chen. Bbn: Bilateral-branch network with cumulative learning for long-tailed visual recognition. In *CVPR*, 2020.

Zhi-Hua Zhou and Xu-Ying Liu. Training cost-sensitive neural networks with methods addressing the class imbalance problem. *IEEE TKDE*, 18(1):63–77, 2005.